

VERY-LOW-PROFILE DUAL-WIDEBAND TABLET DEVICE ANTENNA FOR LTE/WWAN OPERATION

Kin-Lu Wong and Tseng-Wei Weng

Department of Electrical Engineering, National Sun Yat-sen University, Kaohsiung, 80424, Taiwan; Corresponding author: wongkl@ema.ee.nsysu.edu.tw

Received 6 December 2013

ABSTRACT: A simple two-strip antenna formed by a driven strip and a shorted parasitic strip to provide two wide bands with a very low profile of 8 mm for the LTE/WWAN operation (698–960/1710–2690 MHz) in the tablet devices such as a tablet computer is presented. In addition to the very low profile, the antenna occupies a small clearance region of $8 \times 50 \text{ mm}^2$ above the top edge of the device ground plane, and the thickness of the antenna is 3.8 mm only, which is promising for modern tablet device applications. The dual-wideband operation of the antenna is obtained by configuring the driven strip into a step shape, while the shorted parasitic strip includes a main segment and a double-step-shaped shorting segment. The proposed antenna configuration can lead to proper coupling between the driven strip and the parasitic strip, so that wideband resonant modes thereof can be generated, making the antenna's wide higher band cover the desired 1710–2690-MHz band. For the desired lower band of 698–960 MHz, it is achieved by integrating the driven strip with a high-pass matching circuit of a series chip capacitor of 1.8 pF and a parallel chip inductor of 13 nH, which does not increase the antenna's occupied volume and requires no realty space on the device ground plane. The integrated high-pass matching circuit greatly widens the antenna's lower band. Details of the proposed antenna are presented and discussed. © 2014 Wiley Periodicals, Inc. *Microwave Opt Technol Lett* 56:1938–1942, 2014; View this article online at wileyonlinelibrary.com. DOI 10.1002/mop.28487

Key words: mobile antennas; tablet device antennas; LTE/WWAN antennas; very-low-profile antennas; dual-wideband antennas

1. INTRODUCTION

It has been a design challenge for the internal antennas in the tablet communication devices such as the tablet computers to provide two wide operating bands with a very low profile (for example, 8 mm in height only) for the LTE/WWAN (long term evolution/wireless wide area network) operation in the 698–960/1710–2690-MHz bands. The very-low-profile internal LTE/WWAN antenna is very attractive for applications in modern tablet devices, because the spacing or clearance region between the display panel and the device frame thereof can be made narrower so that a more appealing appearance of the tablet device for the users can be obtained.

It is noted that although there have been some interesting low-profile LTE/WWAN tablet device antennas reported recently [1–10], the antenna height above the top edge of the device ground plane is still 10 mm or even 15 mm. To our knowledge for now, there are still no reported internal tablet computer antennas covering the 698–960/1710–2690-MHz bands with a low profile of less than 10 mm. This is mainly because with a decreasing antenna profile, the coupling between the antenna and the device ground plane quickly increases, which makes the antenna's impedance matching difficult to achieve over a wide bandwidth.

In this article, we present a promising internal LTE/WWAN tablet device antenna with a very low profile of 8 mm and a small occupied clearance region of $8 \times 50 \text{ mm}^2$ to cover the 698–960/1710–2690-MHz bands. The antenna has a simple two-

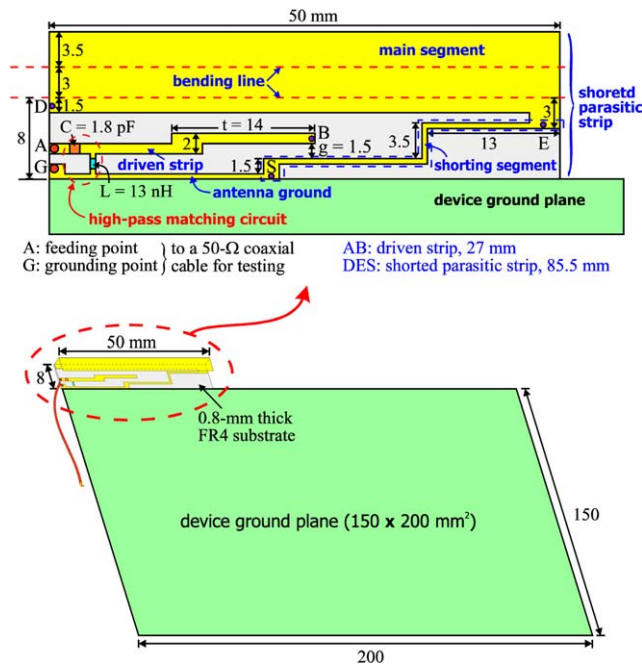


Figure 1 Geometry of the very-low-profile dual-wideband LTE/WWAN tablet device antenna. [Color figure can be viewed in the online issue, which is available at wileyonlinelibrary.com]

strip structure of a driven strip and a shorted parasitic strip, with both configured to achieve proper coupling therebetween such that wideband resonant modes thereof can be generated and formed into a wide higher band for the antenna. For achieving a wide lower band for the antenna, a high-pass matching circuit [11–13] of a series chip capacitor of 1.8 pF and a parallel chip inductor of 13 nH integrated with the driven strip has been found to be effective in the proposed antenna to greatly widen the low-band bandwidth to cover the desired 698–960-MHz band. Furthermore, the integrated high-pass matching circuit does not increase the antenna's occupied volume and requires no realty space on the device ground plane or the system circuit board. This low-band bandwidth enhancement technique compared to the similar techniques such as using a parallel-resonant element [1,14–20] to achieve dual resonance in the antenna's lower band requires less occupied space and is easy to implement. Details of the proposed antenna and its operating principle are presented and discussed.

2. PROPOSED ANTENNA AND ITS OPERATING PRINCIPLE

Figure 1 shows the geometry of the very-low-profile dual-wideband LTE/WWAN tablet device antenna. The antenna has a height of 8 mm and is mounted above the top edge of the device ground plane of dimensions $150 \times 200 \text{ mm}^2$, which is about the ground plane size of a 9.7-inch tablet computer. In the experiment, a copper plate of thickness 0.2 mm is used to simulate the device ground plane (see the fabricated antenna in Fig. 8). The antenna is disposed on a 0.8-mm thick FR4 substrate (relative permittivity 4.4 and loss tangent 0.024) of size $8 \times 50 \text{ mm}^2$ and mounted above the top edge of the device ground plane with a total thickness of 3.8 mm.

The antenna is formed by a driven strip and a shorted parasitic strip. The driven strip is configured as a step-shaped strip of length 27 mm (section AB in the figure) and integrated with a high-pass matching circuit of a series chip capacitor of 1.8 pF (C) and a parallel chip inductor of 13 nH (L). Note that the chip

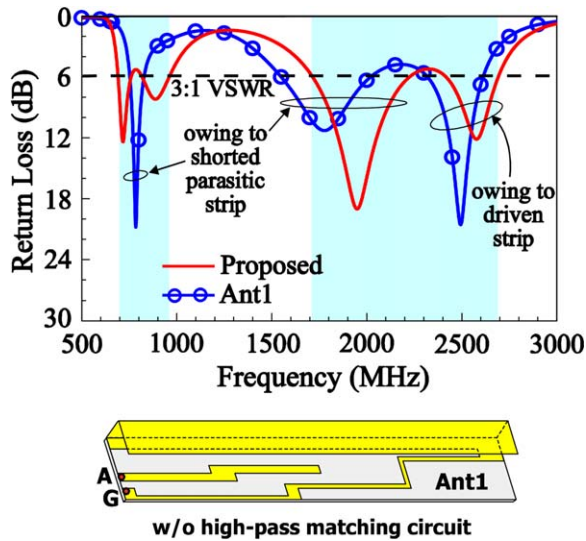


Figure 2 Simulated return loss for the proposed antenna and the case without the integrated high-pass matching circuit (Ant1). [Color figure can be viewed in the online issue, which is available at wileyonlinelibrary.com]

capacitor and inductor are disposed on the FR4 substrate on which the antenna is disposed and does not occupy the realty space on the device ground plane. The driven strip provides a resonant length close to 0.25 wavelength at about 2.5 GHz and can generate a resonant mode in the desired higher band.

The shorted parasitic strip includes a main segment and a double-step-shaped shorting segment. The main segment is bent to occupy a volume of $3 \times 3.5 \times 50 \text{ mm}^3$ to achieve a compact size of the antenna. The main segment is shorted to the antenna ground through the double-step-shaped shorting segment, and the antenna ground is grounded to the device ground plane in the experimental testing. Both the main segment and shorting segment form the shorted parasitic strip, whose length is 85.5 mm and is close to 0.25 wavelength at about 800 MHz. The fundamental resonant mode of the shorted parasitic strip can, hence, occur in the desired lower band. In addition, a higher-order resonant mode of the shorted parasitic strip can occur in the antenna's higher band. Owing to the proper coupling between the driven strip and the shorted parasitic strip in the proposed design, the two resonant modes occurred in the antenna's higher band can be combined to form a wide operating band to cover the desired 1710–2690-MHz band. Also, with the aid of the integrated high-pass matching circuit, an additional resonant mode in the antenna's lower band can be excited to combine with the resonant mode of the shorted parasitic strip to achieve a wide operating band to cover the desired 698–960-MHz band.

Effects of the integrated high-pass matching circuit can be seen clearly in Figure 2, in which the simulated return loss for the proposed antenna and the case without the integrated high-pass matching circuit (Ant1) is shown. The simulated results are obtained using the full-wave electromagnetic field simulator HFSS version 14 [21]. Significant bandwidth enhancement in the antenna's lower band can be seen, which is owing to the presence of the high-pass matching circuit. From the corresponding simulated input impedance for the proposed antenna and Ant1 shown in Figure 3, it is seen that a parallel resonance at about 1.3 GHz occurs owing to the high-pass matching circuit. The center frequency of the parallel resonance can be

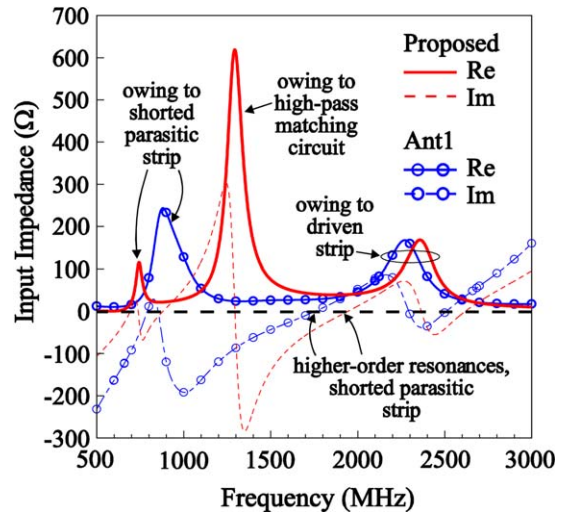


Figure 3 Simulated input impedance for the proposed antenna and Ant1 shown in Figure 2. [Color figure can be viewed in the online issue, which is available at wileyonlinelibrary.com]

tuned by varying the values of the chip inductor and capacitor [11–13]. Also, owing to the parallel resonance, an additional resonance at about 900 MHz is generated, and the impedance variation of the resonant mode contributed by the shorted parasitic strip also becomes smoother. This behavior leads to significant bandwidth enhancement of the antenna's lower band to cover the 698–960-MHz band. For the antenna's higher band, it is seen that two resonant modes contributed by the driven strip and the shorted parasitic strip are combined into a very wide operating band, which covers the 1710–2690-MHz band. Also note that although the return loss for some frequencies in the antenna's lower and higher bands are slightly less than 6 dB, the obtained antenna efficiencies with return loss included (see Fig. 10 in Section 3.) are still acceptable for practical mobile communication applications [1,22].

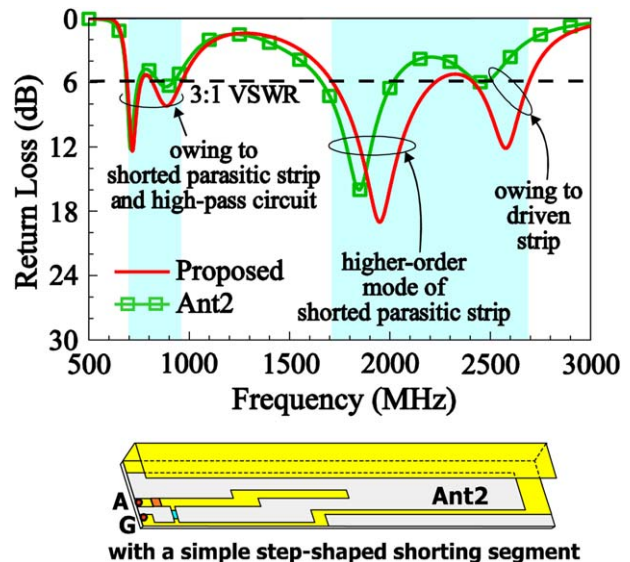


Figure 4 Simulated return loss for the proposed antenna and the case with a simple step-shaped shorting segment in the shorted parasitic strip (Ant2). [Color figure can be viewed in the online issue, which is available at wileyonlinelibrary.com]

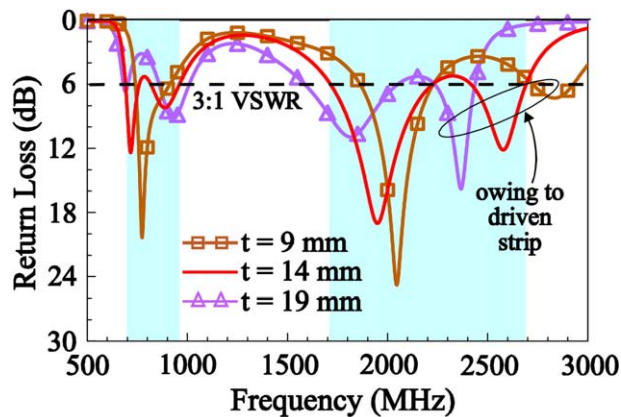


Figure 5 Simulated return loss for the proposed antenna with the driven strip of different lengths. [Color figure can be viewed in the online issue, which is available at wileyonlinelibrary.com]

Effects of the configuration of the shorting segment in the shorted parasitic strip are analyzed with the aid of Figure 4. When a simple step-shaped shorting segment is used (see Ant2 in the figure), relatively large effects on the two resonant modes in the higher band are observed, and better impedance matching for frequencies thereof cannot be obtained. Note that for Ant2 and proposed antenna, the total length of the shorted parasitic strip is about the same. However, by configuring the shorting segment into a double-step shape, the first coupling between the shorting segment and the main segment and the second coupling between the shorting segment and the driven strip can be properly adjusted. This can make the two resonant modes in the antenna's higher band easy to be tuned to form a very wide operating band (see the results of the proposed antenna in Fig. 4).

The dimension and configuration of the driven strip are also important in achieving dual-wideband operation of the proposed antenna. Effects of the simulated return loss for the proposed antenna with the driven strip of different lengths can be seen in Figure 5. When the length t decreases (that is, the total length of the driven strip decreases), the second mode in the higher band is quickly shifted to higher frequencies. In addition, the coupling between the driven strip and the shorting segment will also vary, which greatly affects the two resonant modes (one at about 800 MHz and another at about 2 GHz) contributed by the shorted parasitic strip. Hence, the gap width between the driven strip and the shorting segment is also important, because it can greatly affect the coupling therebetween. Figure 6 shows the simulated return loss as a function of the gap width g between the driven strip and the shorting segment. The obtained results show that the excited resonant modes of the proposed antenna are strongly affected by the gap width g . Hence, by configuring the driven strip into a step shape and the shorting segment into a double-step shape in the proposed antenna, proper coupling between the driven strip and the shorted parasitic strip can be adjusted such that good impedance matching of the excited resonant modes can be obtained over wide operating bands.

Effects of the device ground plane size on the performances of the proposed antenna are also studied. Figure 7 shows the

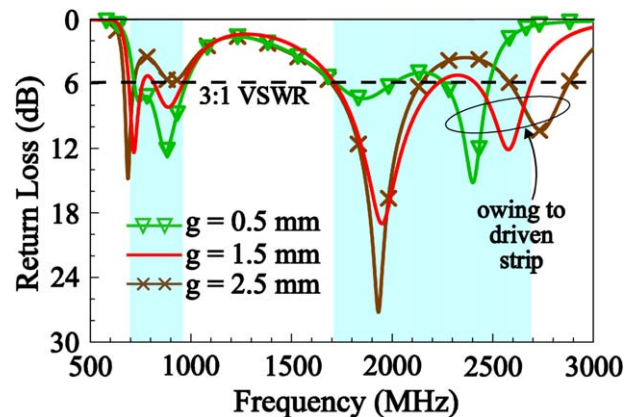


Figure 6 Simulated return loss as a function of the gap width between the driven strip and the shorting segment in the shorted parasitic strip. [Color figure can be viewed in the online issue, which is available at wileyonlinelibrary.com]

simulated return loss for the proposed antenna with different device ground plane sizes. It is interesting to note that slight variations are observed for different device ground plane sizes. This indicates that although the proposed antenna has a very low profile of 8 mm to the device ground plane, the variations in the ground plane sizes will cause negligible effects on the proposed antenna, which makes the proposed antenna easy to apply in practical applications.

3. EXPERIMENTAL RESULTS AND DISCUSSION

The antenna was fabricated and tested. The photos of the fabricated antenna are shown in Figure 8. In the experiment, the antenna was mounted above the top edge of the device ground plane as shown in the photo, and the antenna ground is grounded to the device ground plane. A 50- Ω coaxial line with its central conductor and outer grounding sheath connected, respectively, to point A at the driven strip and point G at the antenna ground was used to feed the antenna. The measured and simulated return losses of the fabricated antenna are shown in

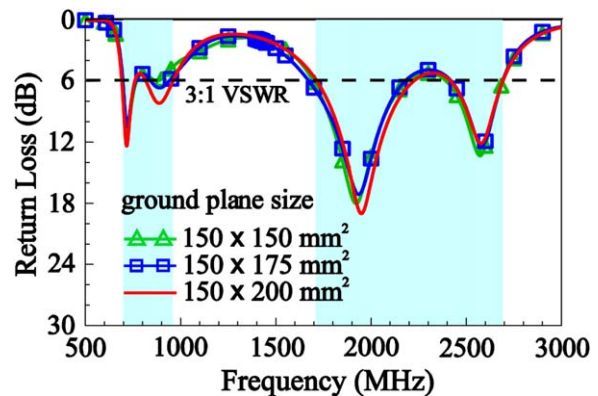


Figure 7 Simulated return loss for the proposed antenna with different device ground plane sizes. [Color figure can be viewed in the online issue, which is available at wileyonlinelibrary.com]

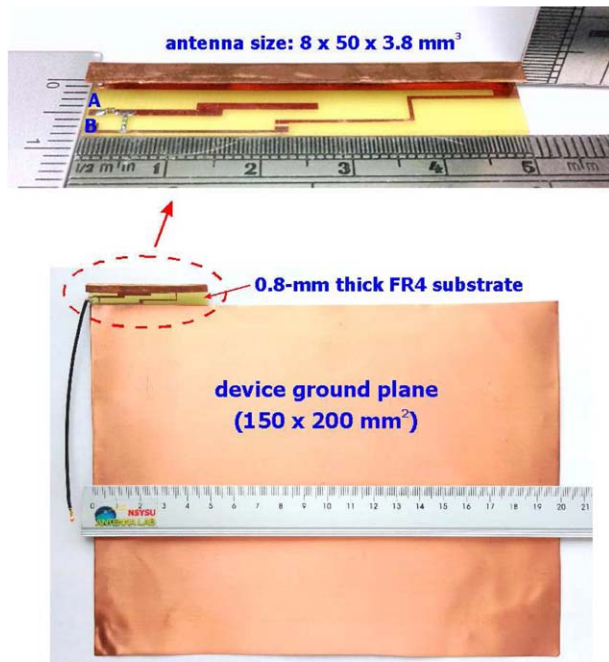


Figure 8 Photos of the fabricated antenna. [Color figure can be viewed in the online issue, which is available at wileyonlinelibrary.com]

Figure 9. Good agreement between the measurement and simulation is obtained. The antenna provides two wide operating bands to cover the desired 698–960 and 1710–2690-MHz bands.

Figure 10 shows the measured and simulated antenna efficiencies of the fabricated antenna, and both include the mismatching losses. Over the lower band, the measured antenna efficiencies are about 42–61%, which is acceptable for practical applications in the mobile devices [1,22]. The relatively large discrepancies between the measured data and simulated results in the high-frequency portion of the lower band, which is close to the excited parallel resonance controlled by the high-pass matching circuit, may be owing to the ohmic losses of the embedded lumped elements. Over the higher band, the measured antenna efficiencies in general agree with the simulated results and are about 64–92%, which is good for practical applications [1,22].

Figure 11 shows the measured and simulated radiation patterns of the fabricated antenna at 850, 1900, and 2500 MHz.

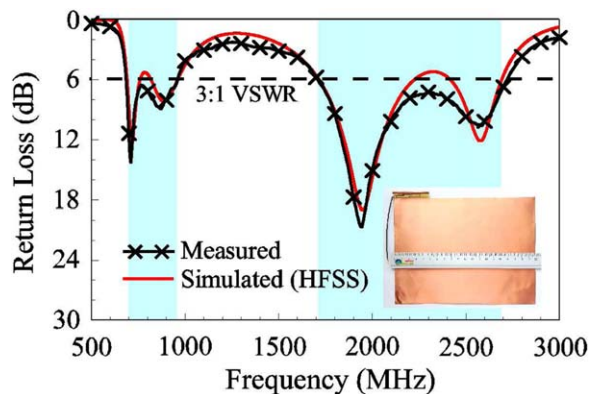


Figure 9 Measured and simulated return losses of the fabricated antenna. [Color figure can be viewed in the online issue, which is available at wileyonlinelibrary.com]

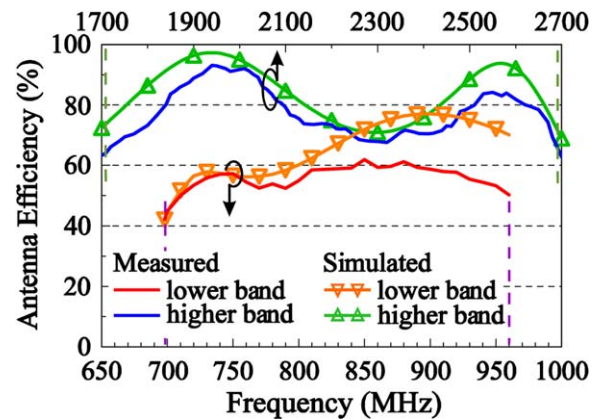


Figure 10 Measured and simulated antenna efficiencies of the fabricated antenna. [Color figure can be viewed in the online issue, which is available at wileyonlinelibrary.com]

Results in three principal planes are plotted, and the radiation intensities in all planes are normalized with respect to the same maximal intensity. The measured data also agree with the simulated results. At 850 MHz (representative frequency in the lower band), near-omnidirectional radiation in the x - y plane is seen. While at 1900 and 2500 MHz (representative frequencies in the higher band), large variations in the radiation patterns are seen. Especially at 2500 MHz, stronger radiation in the upper hemisphere of the y - z and x - z planes is seen, which is different from that observed at 850 or 1900 MHz. This behavior suggests that

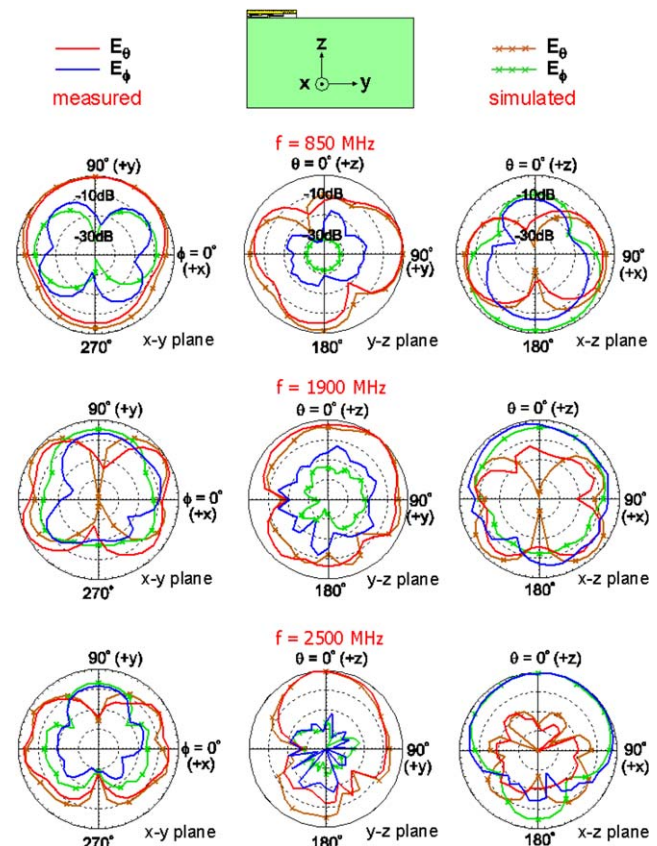


Figure 11 Measured and simulated radiation patterns of the fabricated antenna at 850, 1900, and 2500 MHz. [Color figure can be viewed in the online issue, which is available at wileyonlinelibrary.com]

the device ground plane functions more like a radiator in the lower band and more like a reflector in the higher band, especially in the high-frequency portion of the higher band.

4. CONCLUSION

A very-low-profile dual-wideband tablet device antenna for the LTE/WWAN operation in the 698–960 and 1710–2690-MHz bands has been proposed and studied. The antenna includes a driven strip and a shorted parasitic strip, and both are configured such that proper coupling therebetween can be obtained which leads to wideband resonant modes thereof excited. Also, it has been shown that with the aid of a high-pass matching circuit integrated therein, significant bandwidth enhancement in the antenna's lower band can be obtained. Hence, with the proposed design, the antenna can provide two wide operating bands to cover the whole band of the LTE/WWAN operation with a very low profile of 8 mm and a small occupied volume of $3.8 \times 8 \times 50 \text{ mm}^3$. The proposed antenna is promising for practical applications in modern tablet computers that are with narrow spacing between the display panel and device frame thereof.

REFERENCES

1. K.L. Wong and M.T. Chen, Small-size LTE/WWAN printed loop antenna with an inductively coupled branch strip for bandwidth enhancement in the tablet computer, *IEEE Trans Antennas Propag* 61 (2013), 6144–6151.
2. K.L. Wong and T.W. Weng, Small-size triple-wideband LTE/WWAN tablet device antenna, *IEEE Antennas Wireless Propag Lett* 12 (2013), 1516–1519.
3. W.S. Chen and W.C. Jhang, A planar WWAN/LTE antenna for portable devices, *IEEE Antennas Wireless Propag* 12 (2013), 19–22.
4. Y.L. Ban, S.C. Sun, J.L.W. Li, and W. Hu, Compact coupled-fed wideband antenna for internal eight-band LTE/WWAN tablet computer applications, *J Electromagn Waves Appl* 26 (2012), 2222–2233.
5. S.H. Chang and W.J. Liao, A broadband LTE/WWAN antenna design for tablet PC, *IEEE Trans Antennas Propag* 60 (2012), 4354–4359.
6. K.L. Wong and T.J. Wu, Small-size LTE/WWAN coupled-fed loop antenna with band-stop matching circuit for tablet computer, *Microwave Opt Technol Lett* 54 (2012), 1189–1193.
7. J.H. Lu and Y.S. Wang, Internal uniplanar antenna for LTE/GSM/UMTS operation in a tablet computer, *IEEE Trans Antennas Propag* 61 (2013), 2841–2846.
8. J.H. Lu and F.C. Tsai, Planar internal LTE/WWAN monopole antenna for tablet computer application, *IEEE Trans Antennas Propag* 61 (2013), 4358–4363.
9. K.L. Wong, H.J. Jiang, and T.W. Weng, Small-size planar LTE/WWAN antenna and antenna array formed by the same for tablet computer application, *Microwave Opt Technol Lett* 55 (2013), 1928–1934.
10. K.L. Wong and W.J. Lin, WWAN/LTE printed slot antenna for tablet computer application, *Microwave Opt Technol Lett* 54 (2012), 44–49.
11. M. Tzortzakakis and R.J. Langley, Quad-band internal mobile phone antenna, *IEEE Trans Antennas Propag* 55 (2007), 2097–2103.
12. Z. Zhang, J.C. Langer, K. Li, and M.F. Iskander, Design of ultrawideband mobile phone stubby antenna (824 MHz–6 GHz), *IEEE Trans Antennas Propag* 56 (2008), 2107–2111.
13. K.L. Wong and T.W. Kang, GSM850/900/1800/1900/UMTS printed monopole antenna for mobile phone application, *Microwave Opt Technol Lett* 50 (2008), 3192–3198.
14. S. Jeon, Y. Liu, S. Ju, and H. Kim, PIFA with parallel resonance feed structure for wideband operation, *Electron Lett* 47 (2011), 1263–1265.
15. K.L. Wong, Y.W. Chang, and S.C. Chen, Bandwidth enhancement of small-size WWAN tablet computer antenna using a parallel-resonant spiral slit, *IEEE Trans Antennas Propag* 60 (2012), 1705–1711.
16. K.L. Wong, T.J. Wu, and P.W. Lin, Small-size uniplanar WWAN tablet computer antenna using a parallel-resonant strip for bandwidth enhancement, *IEEE Trans Antennas Propag* 61 (2013), 492–496.
17. K.L. Wong and W.J. Lin, WWAN printed monopole slot antenna with a parallel-resonant slit for tablet computer application, *Microwave Opt Technol Lett* 55 (2013), 40–45.
18. S. Jeon and H. Kim, Mobile terminal antenna using a planar inverted-E feed structure for enhanced impedance bandwidth, *Microwave Opt Technol Lett* 54 (2012), 2133–2138.
19. K.L. Wong and T.J. Wu, Small planar internal WWAN tablet computer antenna, *Microwave Opt Technol Lett* 54 (2012), 426–431.
20. Z. Chen, Y. Ban, S. Sun, and J.L.W. Li, Printed antenna for pentaband WWAN tablet computer application using embedded parallel resonant structure, *Prog Electromagn Res* 136 (2013), 725–737.
21. ANSYS HFSS. Available at: <http://www.ansys.com/products/hf/hfss/>.
22. Z. Li and Y. Rahmat-Samii, Optimization of PIFA-IFA combination in handset antenna designs, *IEEE Trans Antennas Propag* 53 (2005), 1770–1778.

© 2014 Wiley Periodicals, Inc.

A PLANAR RECONFIGURABLE ANTENNA WITH BIDIRECTIONAL END-FIRE AND BROADSIDE RADIATION PATTERNS

Longsheng Liu, Wendong Liu, Yue Li, Zhijun Zhang, and Zhenghe Feng

Department of Electronic Engineering, State Key Lab of Microwave and Communications, Tsinghua University, Beijing 100084, China; Corresponding author: zjzh@tsinghua.edu.cn

Received 8 December 2013

ABSTRACT: *The design of a planar reconfigurable antenna with bidirectional end-fire and broadside radiation patterns from a common aperture is presented in this article. The proposed antenna is composed of two series-feed collinear slot subarrays corporately fed by a microstrip line and two series-feed dipole subarrays corporately fed by a microstrip line-to-double side parallel strip line transition, respectively. A prototype for 2.4 GHz wireless local area networks applications is fabricated and measured. The measured realized gains are about 11–12 and 7–8 dBi for broadside and end-fire patterns. Experimental results, which agree with the simulated ones, verify that the proposed antenna is a good candidate for pattern reconfigurable applications. © 2014 Wiley Periodicals, Inc. *Microwave Opt Technol Lett* 56:1942–1946, 2014; View this article online at wileyonlinelibrary.com. DOI 10.1002/mop.28486*

Key words: *pattern reconfigurable; bidirectional; end-fire; broadside; collinear slot array*

1. INTRODUCTION

With the rapid development of wireless communication, pattern reconfigurable antennas have drawn lots of attention because they enable to provide dynamic radiation coverage, mitigate multipath fading, and improve beam steering capability of phased array systems. In the past decades, there exists an extensive literature on the design of pattern reconfigurable antennas [1–9]. Different methods are used to reconfigure the radiation pattern: one way is selection of different radiating structure including shorting sections [1], parasitic elements [2,3], and antenna shape [4], or adjustment of radiating elements [5,6], another is switching between different feed networks [7–9].

In this article, a two-port pattern diversity antenna providing bidirectional end-fire and broadside radiation patterns from a